CHAPTER VII
COMBINED STEAM REFORMING AND PARTIAL OXIDATION OF METHANE TO SYNTHESIS GAS UNDER ELECTRICAL DISCHARGE

7.1 Abstract

An experimental study of synthesis gas production from simultaneous steam reforming and partial oxidation of methane using an ac corona discharge was conducted. The benefits of the combination of the two reactions reduce the pure oxygen requirement in the system and increases thermal efficiency by transferring heat between the exothermic and endothermic reactions. The results show that the addition of water-vapor greatly enhanced the conversions of methane and oxygen and improved the energy efficiency in an oxygen-lean system. The energy consumed to convert a methane molecule decreased dramatically from 68 to 13 eV/m_c with increasing percentage of water-vapor from 0 to 50% at a CH_4/O_2 ratio of 2. At the conditions studied, input power had more influence on the methane and oxygen conversions than applied frequency.

7.2 Introduction

Synthesis gas, consisting of hydrogen and carbon monoxide, is an important raw material in chemical manufacture such as e.g. Fischer-Tropsch synthesis to produce higher hydrocarbons (reaction 7.1), methanol synthesis (reaction 7.2) and hydrogen synthesis[1]. Additional hydrogen can be produced from synthesis gas by transformation of carbon monoxide in the water gas shift reaction (reaction 7.3) followed by carbon dioxide removal[2].

$$nCO + 2nH_2 \rightarrow C_nH_{2n} + nH_2O \quad (7.1)$$

$$CO + 2H_2 \rightarrow CH_3OH \quad (7.2)$$

$$CO + H_2O \rightarrow CO_2 + H_2 \quad (7.3)$$

The primary method of synthesis gas production has been steam reforming, shown in reaction 7.4. It is very useful to use low cost materials to produce synthesis gas and most existing synthesis gas plants use a steam and natural gas mixture via the steam reforming reaction over a Ni catalyst at high temperatures (>900 °C). The catalyst is placed in alloy tubes arranged inside a furnace with the heat of the highly endothermic reaction supplied by burners[2]. Expensive alloys are needed to tolerate the extremely high thermal fluxes through the tube walls[3] and to reduce potential issues of metal dusting caused by carbon monoxide production[4]. Though much energy can be recovered, it is as lower quality heat. The tendency for carbon deposition on the catalyst can also be one of its drawbacks. Consequently, steam reactors are usually operated with a higher H_2O/CH_4 ratio than the stoichiometric value. This results in higher H_2/CO ratios (in the range of 3.4-5.0) than required for Fischer-Tropsch synthesis and methanol production and the high ratio of H_2/CO also would limit the carbon chain growth in Fischer-Tropsch synthesis[5,6]. The H_2/CO ratio that is obtained from steam reforming must be adjusted by the reverse water gas shift reaction or the purging of hydrogen for use as a supplemental fuel or downstream reactant[6].

Partial Oxidation of methane is another way to produce synthesis gas and gives a H_2/CO ratio of 2 as shown in reaction 7.5. Non-catalytic partial oxidation of methane occurs only at very high temperatures. Much research has been focused on the partial oxidation of methane over different catalysts[7-12]. Although several catalysts are active for this reaction, a significant problem is rapid deactivation. Undesirable carbon formation cannot be avoided by increasing the O_2/CH_4 ratio as well as the operating temperature leading to the potential explosion hazards, separation problems, gas phase reactions and a decrease in the synthesis gas selectivity[5]. Though the need of using pure oxygen as the feed gas has high investment and operating cost, this appears to be favored for several new commercial Fischer-Tropsch process designs.

$$CH_4 + H_2O \rightarrow CO + 3H_2 \qquad (7.4)$$

$$CH_4 + \tfrac{1}{2}O_2 \rightarrow CO + 2H_2 \qquad (7.5)$$

A combination of non-catalytic partial oxidation and steam reforming has a benefit in term of balancing the heat load. Methane conversions can be achieved up to 90% with residence times of up to 0.1 s. However, a typical steam reforming with oxygen reactor operates at about 2,200 K in the combustion zone and 1,200-1,400 K in the catalytic zone[13]. Many researchers have studied steam reforming with oxygen to improve its efficiency. A possible improvement of this reaction is operation under a low temperature plasma environment.

The use of plasma chemistry based technologies started as high temperature equilibrium plasma processes for production of carbon, black, acetylene and hydrogen, but power costs are quite high. It was found that a low temperature non-equilibrium plasma has benefits for some technologies because of its non-equilibrium properties[14]. The unique characteristic of the non-equilibrium plasma is that its electrons reach high temperatures of 10,000 to 100,000 K (1-10 eV) while the bulk gas temperature remains close to ambient temperature. Consequently, the low gas temperature of the plasma, while achieving high feed conversions, can allow selectivity control for the desired products[14] as well as result in lower power consumption and much less need for waste heat recovery.

A non-equilibrium discharge is an effective tool to generate energetic electrons, which can initiate a series of plasma chemical reactions such as ionization, dissociation, and excitation. Utilization of non-equilibrium plasmas as a "catalytic initiator" offers several potential advantages for chemical synthesis processes such as low cost, high selectivity, and fewer pollutants compared with other processes. It is a high productivity volumetric process, e.g. the interaction between accelerated charged particles (i.e. electrons and ions) and other chemical species (i.e. molecules and radicals) takes place in the whole plasma volume to promote the reaction, which is not possible in surface catalytic technologies[15]. Using electric discharges not only may provide heat to the reaction, but also can initiate species in the homogeneous phase to speed up elementary reactions[2].

Non-equilibrium plasmas have been extensively studied as a possible way to initiate the reaction of methane to form various products for industrial application because of their effectiveness in the activation of methane at low gas temperatures and atmospheric pressure[16-21]. It is also of interest to find ways to improve synthesis

gas production from methane by using electric discharges[2,22]. Also, it has been found that the energy consumption in this system is in the same range as net energy consumption for Fischer Tropsch synthesis (~320 kWh/1000scf), and a simpler process may result. Applications for corona discharge processes have existed for over a hundred years. The corona discharge plays an important role in several industrial applications such as electrostatic precipitation, electro photography, static control in semiconductor manufacture, ionization instrumentation, generation of ozone, and destruction of toxic compounds. Some of these applications were reviewed by Jen-Shih Chang et al.[23].

In this paper, combined steam reforming and partial oxidation of methane to synthesis gas under corona discharge has been studied to investigate the operational parameters, i.e. feed gas composition, residence time, applied frequency and input power, affecting methane conversion, product distribution and energy consumption.

7.3 Experimental

The corona discharge was created in a reactor which consisted of a quartz tube with an inside diameter of 7.0 mm. The schematic diagram of the system is shown in Figure 7.1. The plasma was formed in the gap between two stainless steel electrodes that had a gap distance between the two of 10 mm. The lower electrode was a circular plate, which was mounted perpendicular to the tube axis with holes in it to allow gas to pass through the reactor. The upper electrode was a wire suspended and centered axially within the reactor tube. All the experiments were conducted at atmospheric pressure. The flow rates of feed gases were regulated by mass flow controllers (Porter Instrument Co., Model 201). Water-vapor was introduced into the reactor by passing the feed mixture of methane and oxygen through a bubbler in which the temperature was controlled to adjust the concentration of water-vapor in the feed gas mixture. The average water mole fraction was confirmed by measuring the mass of water vaporized during the experiment. The feed gases were well mixed and then flowed downward through the reactor. The temperatures of the reactor and gas lines were maintained at 100 °C to avoid condensation of water-vapor. The exhaust gas from the reactor was introduced into a condenser cooled by a mixture of

dry ice and acetone to remove water and liquid organic products. However, liquid organic products were not found when analyzed with a Varian 3300 GC with a Porapak Q column. The compositions of the feed gas mixture and the outlet gas were quantitatively measured by an on-line gas chromatograph (HP 5890) with a thermal conductivity detector (TCD). The flow rates of the outlet gas were also measured by using soap bubble flow meter.

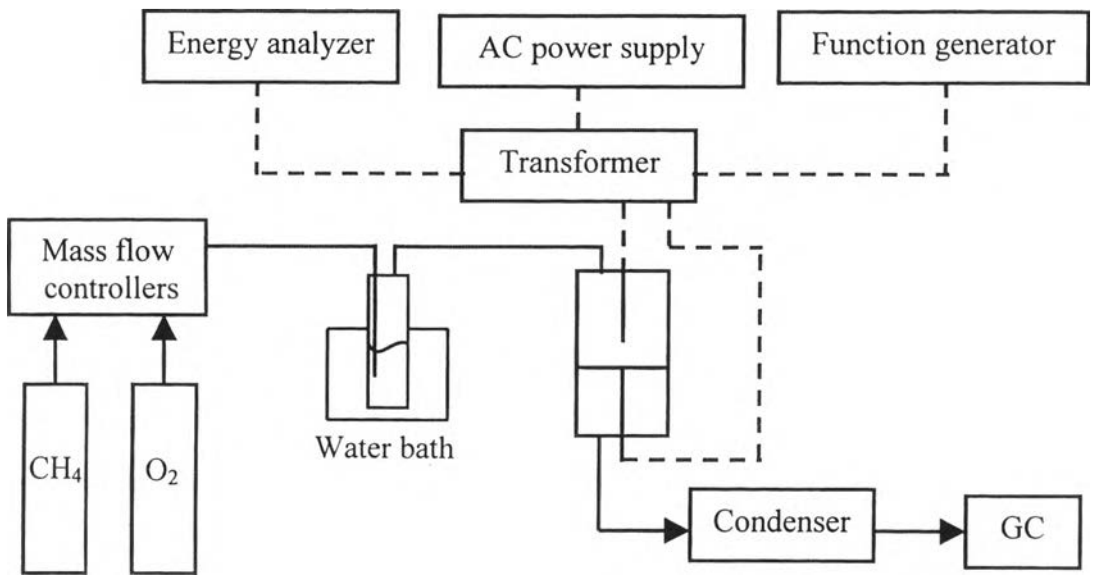

Figure 7.1 Schematic diagram of corona discharge reactor.

The AC power source consisted of an AC power supply, multifunction generator and transformer. The domestic AC input of 120 Volts and 60 Hz was supplied through an Elgar AC power supply. A multifunction generator was used in conjunction with the power supply to form a sinusoidal waveform at the desired frequency. The output of the power supply was transmitted to a high voltage (HVAC) transformer for stepping up the low side voltage to the high side voltage by a nominal factor of 125 at 60 Hz and then supplied to the reactor. An Extech power analyzer was used to measure the power, power factor, current, frequency, and voltage at the low voltage side of the power circuit.

For this system, the conversions were defined as:

Conversion of methane = (moles of CH_4 consumed/moles of CH_4 introduced) × 100 %

Conversion of oxygen = (moles of O_2 consumed/moles of O_2 introduced) × 100 %

The computation of selectivities were based on carbon converted as:

% Product selectivity = (total number of moles of carbon formed/total number of moles of carbon reacted) × 100 %

H_2/CO mole ratio = moles of H_2 produced/moles of CO produced

CO/C_2 mole ratio = moles of CO produced/moles of ethane, ethylene and acetylene produced

The total carbon selectivity of products containing carbon atom was typically about 90 percent. However, no deposition of carbonaceous solid was observed inside the reactor throughout all experiments for the conditions studied. The "loss" of carbon probably resulted from experimental error. The residence time was calculated based on the volume of the reactor between the two electrodes. The energy consumed to convert a methane molecule (eV/m_c) was calculated using input energy in terms of electron-volts (eV) per converted methane molecule and included power losses from the all of the power equipment. For reference, $1 eV/m_c$ amounts to about 31 kWh/1000scf of methane.

A "standard" experiment for this study encompasses the following conditions, from which paramter variations were made as discussed in the various results sections. The reactor had a gap width and residence time of 10 mm and 0.23 s, respectively at a constant input power and applied frequency of 11 W and 300 Hz. The CH_4/O_2 ratio was kept constant of 5 while adding 30% water-vapor in feed gas. The experiment could be reproduced with results within 7%.

7.4 Results and Discussion

7.4.1 Effect of Feed Gas Composition

The first experiments were performed to investigate the effect of feed gas composition. Three CH_4/O_2 ratios of 2, 3, and 5 were used with varying water-vapor contents of 0, 10, 30, and 50% of the total feed gas flow rate. The results, shown in Table 7.1, indicate that feed gas composition is a significant parameter affecting both conversions and product distribution. Increasing the CH_4/O_2 ratio leads to rapid decreases in both methane and oxygen conversions resulting from reduction of oxygen availability in the system due to oxygen's importance in methane activation. Similar results in both dielectric barrier discharges and corona discharges have been reported[16,18,24,25].

Pure methane cannot be easily activated in the corona discharge because the ionization potentials of methane are greater than 12 eV[26], higher than the average electron energy produced from the corona discharge used here. Due to its electronegative nature, oxygen relatively easily forms negative ions in the discharge. A number of possible pathways to activate oxygen molecules are shown in the following reactions[24]:

Dissociative attachment :

$$e^- + O_2 \rightarrow 2O + e^- \rightarrow O^- + O \qquad (7.6)$$

Attachment :

$$e^- + O_2 \rightarrow O_2^- \qquad (7.7)$$

Dissociation :

$$e^- + O_2 \rightarrow 2O + e^- \qquad (7.8)$$

The electrons produced in a corona discharge, with average electron energy of about 5 eV, are sufficient to activate oxygen molecules by dissociative attachment, that requires the least energy in comparison with the other reactions[27,28].

Table 7.1 Effect of feed gas composition on conversions and product distribution; gap width, 10 mm; residence time, 0.23 s; input power, 11 W; and applied frequency, 300 Hz.

CH_4/O_2 Ratio	Water (%)	Conversion (%)		Selectivity (%)					H_2/CO	CO/C_2
		CH_4	O_2	CO	CO_2	C_2H_2	C_2H_4	C_2H_6		
2	0	49	83	62	10	13	11	3	1.6	4.6
	10	46	86	57	8	16	11	3	1.7	3.8
	30	51	77	59	8	17	9	3	1.9	4.1
	50	40	57	62	8	16	10	3	2.0	4.3
3	0	19	40	47	10	8	20	11	2.2	2.4
	10	22	45	48	9	10	21	11	2.2	2.3
	30	30	52	47	5	18	15	6	2.5	2.4
	50	36	62	57	6	23	13	5	2.7	2.8
5	0	4	9	13	10	0	14	45	4.2	0.6
	10	8	13	23	4	6	19	25	3.6	0.9
	30	18	33	33	3	23	19	11	4.0	1.2
	50	30	55	39	3	28	13	5	3.8	1.7

In this corona discharge, CH_4 is evidently activated by hydrogen abstraction to form CH_3, CH_2, CH, and C consecutively by active oxygen species leading to a significant rate of methane conversion in the corona discharge. These CH_3, CH_2 and CH may couple to form ethane, ethylene, and acetylene, respectively (reactions 7.9-7.11, noting in addition that there is coupling to form radicals that can decompose to form the stable species containing less hydrogen, e.g. $CH_2 + CH_3 \rightarrow C_2H_5 \rightarrow C_2H_4 + H$). Additionally, ethane can be dehydrogenated to form ethylene and ethylene is then dehydrogenated to form acetylene (overall reactions 7.12-7.13). Hydrogen may form predominantly via hydrogen abstraction by H. The maximum ethane selectivity was found at a CH_4/O_2 ratio of 5 while the maximum carbon monoxide was found at CH_4/O_2 ratio of 2. The oxidation of methane to carbon oxides and water is more favored at higher oxygen concentrations. A higher CH_4/O_2 ratio, with less oxygen, increases the probability of an activated C_1 species reacting with another carbon containing to produce C_2s and decreases the probability of an activated C_1 or C_2 species reacting with active oxygen species resulting in decreased production of other CH_X species and carbon oxides. For this reason, ethane selectivity increases but the CO/C_2 ratio decreases with increasing CH_4/O_2 ratio.

$$CH_3 + CH_3 \rightarrow C_2H_6 \qquad (7.9)$$

$$CH_2 + CH_2 \rightarrow C_2H_4 \qquad (7.10)$$

$$CH + CH \rightarrow C_2H_2 \qquad (7.11)$$

$$C_2H_6 \rightarrow C_2H_4 + H_2 \qquad (7.12)$$

$$C_2H_4 \rightarrow C_2H_2 + H_2 \qquad (7.13)$$

At a CH_4/O_2 ratio of 2, adding water-vapor to the feed gas had a negative effect on the conversions of methane and oxygen. The methane and oxygen conversions dramatically decreased while the product selectivities were not changed significantly with increasing water-vapor content. However, adding water-vapor to the feed at higher CH_4/O_2 ratios gave different results. At CH_4/O_2 ratios of 3 and 5, a positive effect on conversions of both methane and oxygen when adding water-vapor

was observed. Ethane selectivity decreased while carbon monoxide selectivity increased with increasing water content in an oxygen-lean system. It can be concluded that increasing water content at a constant high CH_4/O_2 ratio of 3 and 5, shows a similar trend for conversions and selectivities as decreasing the CH_4/O_2 ratio at constant water content. The conversions and product distribution depended more on water-vapor content at the CH_4/O_2 ratio of 5 than at the CH_4/O_2 ratio of 3.

The main effect of water content in this plasma system is to changes in the distribution of active species and therefore pathways. Water plays an important role in supplying active species, i.e. OH, H, and O, from its dissociation reactions with relatively low electron energy within the plasma as shown in reactions 7.14-7.15[29]. These active species can activate methane to form other products by increasing the rate of formation of methyl radicals (reactions 7.16-7.18). Consequently, methane conversion increases with increasing water content. At a CH_4/O_2 ratio of 2, oxygen species are relatively "plentiful" in the reactor. Adding active species to the system, which has" enough" active oxygen species, is not an effective way to enhance the methane conversion because of the dilution of methane. In addition, the product pathways do not change substantially with increased active species in the system because the system already has relatively abundant oxygen. The previous mention about the effect of CH_4/O_2 feed mole ratio on reaction pathways is also consistent with the effect of water content on selectivity since dissociation of water also gives active oxygen species. For CH_4/O_2 ratios of 3 and 5, the selectivities of carbon monoxide, acetylene, and the CO/C_2 ratio increase, but ethane, ethylene and carbon dioxide selectivities decrease. These results suggest that active species from dissociation of water enhance secondary reactions of dehydrogenation and oxidation. The experiments also showed that the product distribution was slightly dependent on the water-vapor content but strongly dependent on CH_4/O_2 ratio. Thus a change of CH_4/O_2 ratio more strongly affects the oxygen active species in the system than the change in water content.

$$e^- + H_2O \rightarrow O^- + H_2 \qquad (7.14)$$

$$e^- + H_2O \rightarrow OH^- + H \quad (7.15)$$

$$CH_4 + O^- \rightarrow CH_3 + OH^- \quad (7.16)$$

$$CH_4 + H \rightarrow CH_3 + H_2 \quad (7.17)$$

$$CH_4 + OH \rightarrow CH_3 + H_2O \quad (7.18)$$

Figure 7.2 shows the effect of feed gas composition on energy consumed to convert a methane molecule. Decreasing the CH_4/O_2 ratio decreased the energy consumed to convert a methane molecule without significantly changing the electrical properties. This indicates that active oxygen species enhance energy efficiency of the system by their facilitation of methane conversion and decreasing the energy consumed in converting a methane molecule. At a CH_4/O_2 ratio of 5, the energy consumed to convert a methane molecule decreased dramatically from 68 to 13 eV/m_c with increasing percentage of water-vapor from 0 to 50, indicating that significant active oxygen species may be generated from water. However, the energy consumed to convert a methane molecule is constant with increasing water-vapor at a CH_4/O_2 ratio of 3. For a CH_4/O_2 ratio of 2, adding water-vapor not only reduced methane conversion but also reduced the energy efficiency slightly. It can be concluded that active species from dissociation of both oxygen and water remarkably enhance energy efficiency of the system. However, high fractions of these oxygen containing species increases the energy consumed to convert a methane molecule since some of them absorb energy without collision with methane molecules and the lower throughput of methane. It is possible to control the composition of synthesis gas and optimize the efficiency of system by adjusting the feed gas composition.

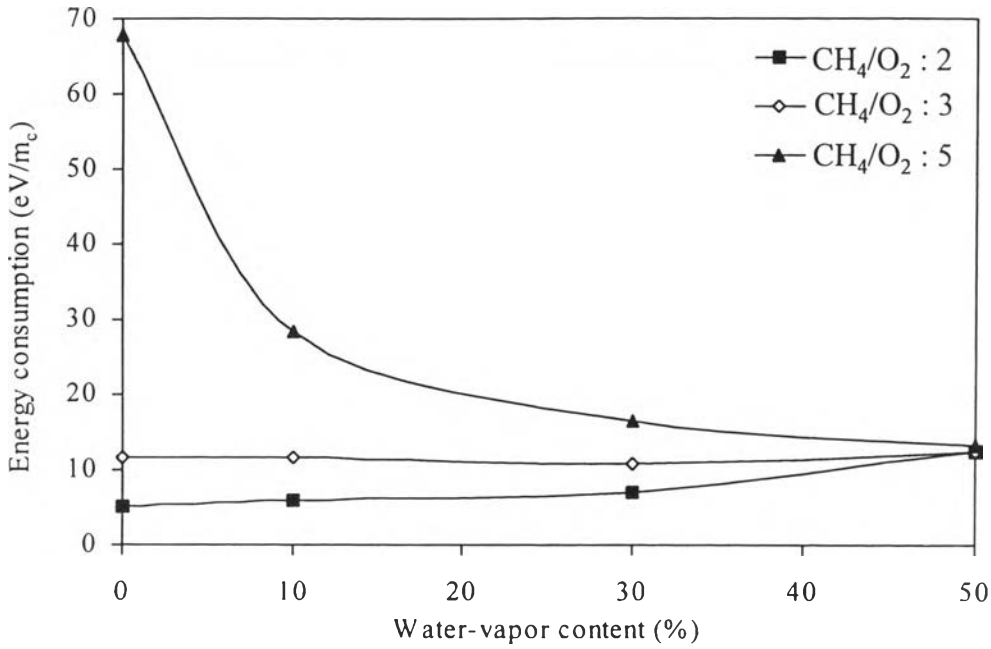

Figure 7.2 Effect of feed gas composition on energy consumed to convert a methane molecule; gap width, 10 mm; residence time, 0.23 s; input power, 11 W; and applied frequency, 300 Hz.

7.4.2 Effect of Applied Power

Table 7.2 shows the effect of applied power in the ac corona discharge on methane reforming with oxygen and water-vapor. The experiments were performed at three conditions with the same water-vapor content of 30%. The first condition, condition A, was at a residence time of 0.23 s, CH_4/O_2 ratio of 5, and frequency of 300 Hz. The second condition, condition B, was operated at the same condition as condition A except for a CH_4/O_2 ratio of 3. The last condition, condition C, was performed at a residence time, frequency, and CH_4/O_2 ratio of 0.06 s, 400 Hz, and 5, respectively. The power was increased from the lowest power that the discharge could be sustained to the highest power that could be operated without carbon formation. Conditions A and B were operated at nearly the same power range. Condition C was operated at a higher power to increase conversion since the residence time was shorter. The relation between input power and residence time will be discussed more clearly in the section on the effect of residence time.

Table 7.2 Effect of power on conversions and product distribution; gap width, 10 mm; and percentage of water-vapor, 30.

Condition A: CH_4/O_2 ratio, 5; applied frequency, 300 Hz; residence time, 0.23 s

Condition B: CH_4/O_2 ratio, 3; applied frequency, 300 Hz; residence time, 0.23 s

Condition C: CH_4/O_2 ratio, 5; applied frequency, 400 Hz; residence time, 0.06 s

Condition	Power (W)	Conversion (%)		Selectivity (%)					H_2/CO	CO/C_2
		CH_4	O_2	CO	CO_2	C_2H_2	C_2H_4	C_2H_6		
A	11	18	33	33	3	23	19	11	4.0	1.2
	13	22	49	35	4	17	19	9	3.5	1.5
	15	24	56	37	6	18	19	9	3.4	1.6
	16	24	59	35	6	18	18	8	3.6	1.6
B	9	24	31	40	3	18	16	9	2.8	1.9
	11	30	52	47	5	18	15	6	2.5	2.4
	13	33	60	51	6	18	15	6	2.4	2.7
	14	34	65	50	7	18	14	5	2.5	2.7
	16	38	72	49	9	18	12	4	2.5	2.8
C	14	9	7	32	2	40	11	6	5.0	1.1
	16	11	14	33	2	38	11	6	4.9	1.2
	18	13	20	33	3	38	12	6	4.8	1.2
	20	14	18	32	4	37	11	6	4.9	1.2
	22	16	16	30	4	37	11	6	4.7	1.2

It was found experimentally that methane and oxygen conversions increased with applied power at all conditions. The energies of individual electrons produced in the reactor are not the same, but have a distribution. Only sufficiently high-energy electrons can activate a particular molecule to form a *reactive*-active species[20]. For the same reactor geometry, pressure, and gas, increasing power increases the number of electrons at each energy level within the same distribution. An increase in current, or number of electrons over time, with increasing power, shown in Figure 7.3, also confirms this explanation. In other words, the density of electrons with sufficient energy to activate molecules in the reactor increases with increasing power, resulting in increasing methane and oxygen conversions. For condition B, performed with higher oxygen content in the feed stream, increasing methane and oxygen conversions were higher than those in conditions A and C when the power was increased. In the system with higher oxygen partial pressure, oxygen has a greater probability of colliding with electrons to form active oxygen species and these active species may further activate methane molecules. At higher power, methane has a greater probability of being activated to form CH_2 and CH than CH_3. Furthermore CH_2 and CH are more reactive than CH_3 in the presence of oxygen and the main products would be carbon oxides and/or ethylene and acetylene[21]. Acetylene can be formed directly from CH_2 and CH or from dehydrogenation of ethane and ethylene since the system has sufficient high-energy electrons and reactive H atoms to dehydrogenate ethane to produce ethylene and then acetylene. The C_2s can undergo further oxidation to carbon monoxide and carbon dioxide. As can be seen in Table 7.2, for conditions A and B, the CO/C_2 product ratio increases with increasing power. This shows that the secondary reaction of oxidation increases with increasing power. The selectivity change of condition B is larger than condition A. An explanation is that for condition B, the oxygen conversion increase is higher than the methane conversion increase with increasing power resulting in a shift in the balance between reaction pathways. However, for condition C, product selectivities are nearly constant, resulting in a constant CO/C_2 at about 1.2. Because condition C was operated at short residence time, the primary products have less time to react with active species to undergo secondary reactions. The results from this study suggest that under conditions with a sufficient source of activated oxygen, the

secondary reactions of dehydrogenation and oxidation become predominant with increasing power.

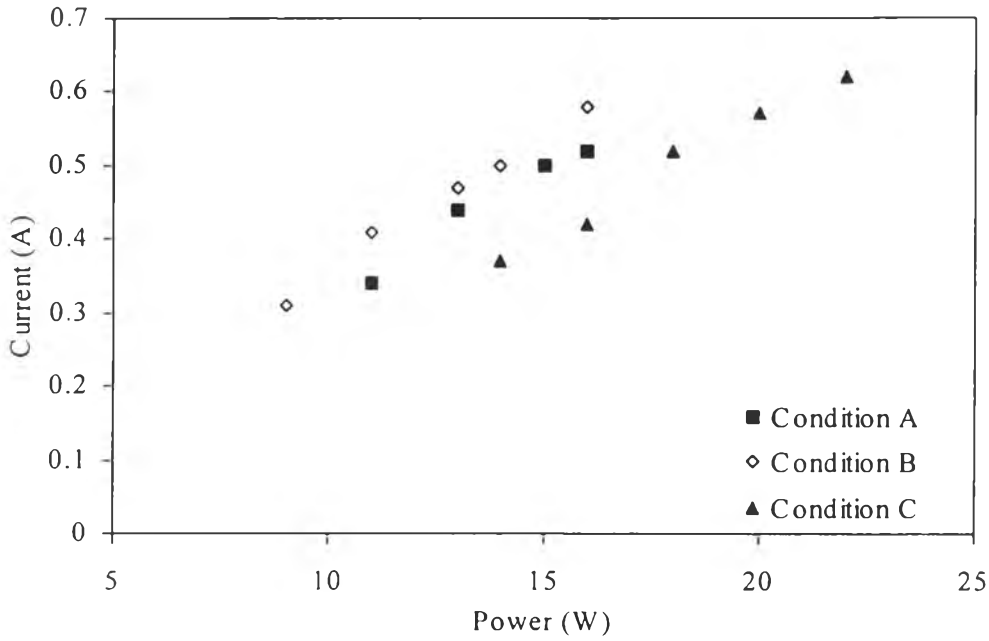

Figure 7.3 Effect of power on current; gap width, 10 mm; and percentage of water-vapor, 30.

Condition A: CH_4/O_2 ratio, 5; applied frequency, 300 Hz; residence time, 0.23 s

Condition B: CH_4/O_2 ratio, 3; applied frequency, 300 Hz; residence time, 0.23 s

Condition C: CH_4/O_2 ratio, 5; applied frequency, 400 Hz; residence time, 0.06 s

The energy consumed to convert a methane molecule is relatively constant with increasing power as shown in Figure 7.4. This indicates that the methane conversion increases linearly with increasing power in this conversion range. For all three conditions, A, B, and C, the optimal input power is the highest power that can be operated without carbon formation. At the optimal input power, the maximum methane conversion is reached with the same energy efficiency as at other input power.

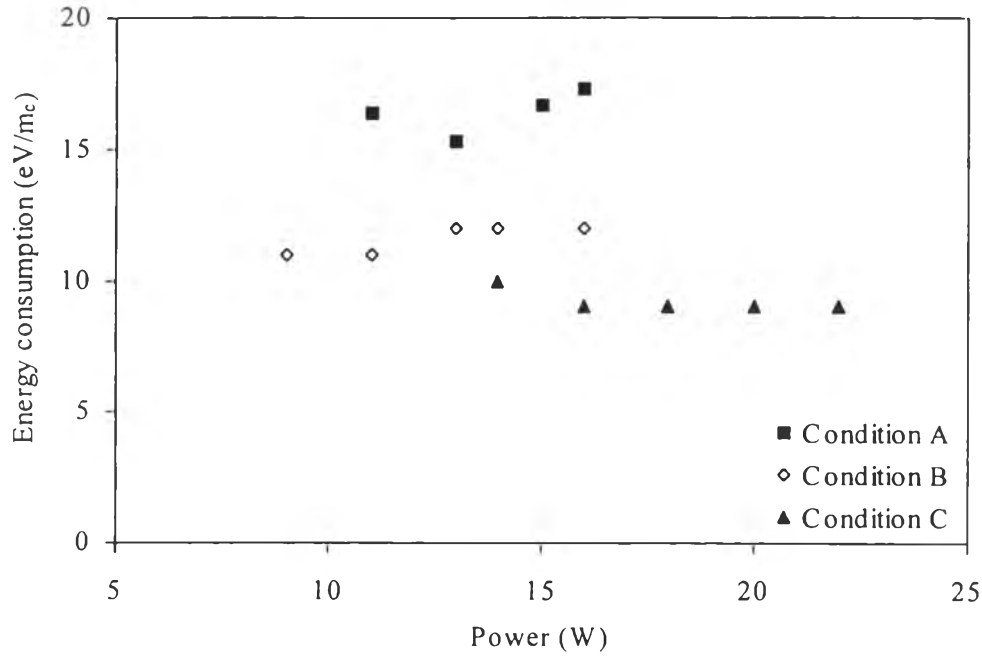

Figure 7.4 Effect of power on energy consumed to convert a methane molecule; gap width, 10 mm; and percentage of water-vapor, 30.
Condition A: CH_4/O_2 ratio, 5; applied frequency, 300 Hz; residence time, 0.23 s
Condition B: CH_4/O_2 ratio, 3; applied frequency, 300 Hz; residence time, 0.23 s
Condition C: CH_4/O_2 ratio, 5; applied frequency, 400 Hz; residence time, 0.06 s

7.4.3 Effect of Frequency

The results of methane reforming with oxygen and water-vapor at different applied frequencies are shown in Table 7.3. The percent water-vapor in the feed mixture was at 50 or 30%, while the methane to oxygen ratio was kept constant at 5. The methane and oxygen conversions exhibited a maximum at a frequency of around 400 Hz. As the ac discharge is applied, the streamer corona discharge is thought to be a temporary DC corona discharge, each electrode performing alternately as anode or cathode[24]. The alternation of the electric field probably reduces and inhibits the accumulation of contaminants on the electrode surface as well as on the quartz tube wall[24]. The highest currents, of 0.35 and 0.37 A at 30% and 50% water-vapor in feed gas, respectively, are found at a frequency of 400 Hz, as shown in Figure 7.5. At the highest current, there were the largest numbers of electrons available to activate methane to produce all products resulting in maximum methane and oxygen conversions. Beyond 400 Hz, the current decreases with

increasing frequency. At 300 Hz, the current was slightly lower than the current at 400 Hz. The discharge turned to an arc discharge and carbon was observed in the reactor when the frequency was decreased lower than 300 Hz. The reaction has to be operated at "*carbon-free*" condition to have a significant reactive volume. Since this carbon is electrically conductive, the current tends to flow almost entirely through these carbon deposits. This reduces the number of discharge streamers and limits the number of energetic electrons that can interact with the feed gases in the reaction zone resulting in a reduction of methane conversion as well as the reaction rate. Decreases in both current and conversions of methane and oxygen when the frequency was decreased from 400 to 300 Hz are probably due to the initiation of carbon formation in the reactor resulting in changing the plasma characteristics. The product distribution did not change significantly with changes in frequency because methane and oxygen conversions change at the same rate with varying frequency. It can be concluded that decreasing the frequency increases methane conversion without a change of reaction pathway. Figure 7.6 shows the minimum energy consumed to convert a methane molecule was found at 400 Hz, the same frequency with maximum methane conversion. We may conclude that the optimum frequency for this system is about 400 Hz. For the conditions studied, the frequency had little influence on methane conversion and energy consumed to convert a methane molecule in comparison with input power.

Table 7.3 Effect of frequency on conversions and product distribution; gap width, 10 mm; residence time, 0.23 s; CH_4/O_2 ratio, 5; and input power, 11 W.

Water (%)	Frequency (Hz)	Conversion (%)		Selectivity (%)					H_2/CO	CO/C_2
		CH_4	O_2	CO	CO_2	C_2H_2	C_2H_4	C_2H_6		
30	300	18	33	33	3	23	19	11	4.0	1.2
	400	22	38	33	3	25	18	9	4.0	1.3
	500	21	40	32	3	25	19	10	4.2	1.2
	700	18	27	34	2	31	18	11	4.5	1.2
50	300	30	55	39	3	28	13	5	3.8	1.7
	400	35	55	39	3	28	12	5	3.8	1.7
	500	30	51	40	3	29	12	6	3.8	1.7
	700	29	40	37	2	27	11	6	3.9	1.6

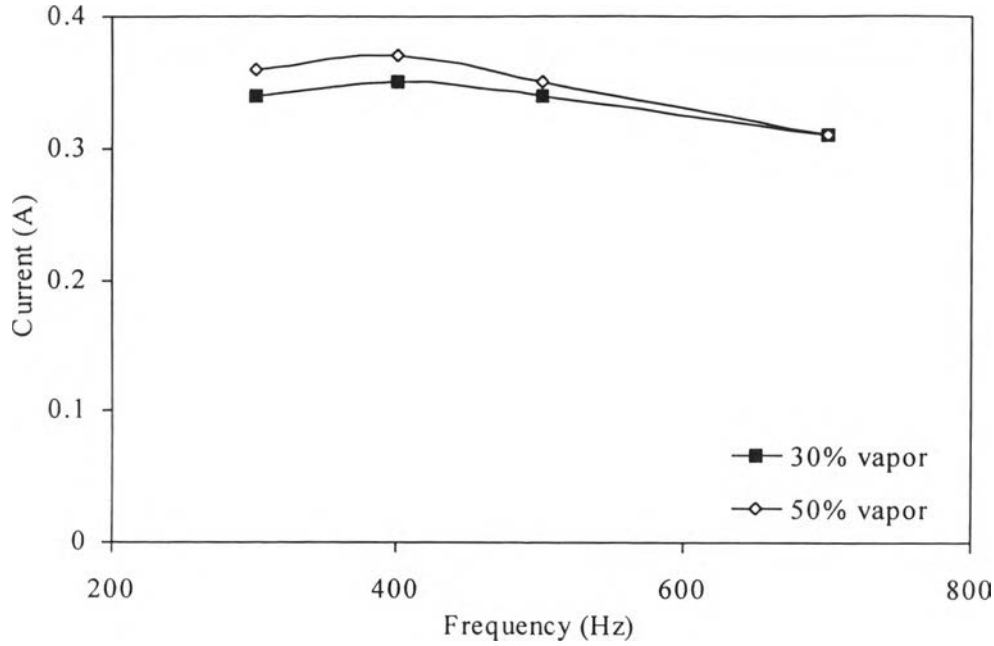

Figure 7.5 Effect of frequency on current (conditions are the same as those in Table 7.3).

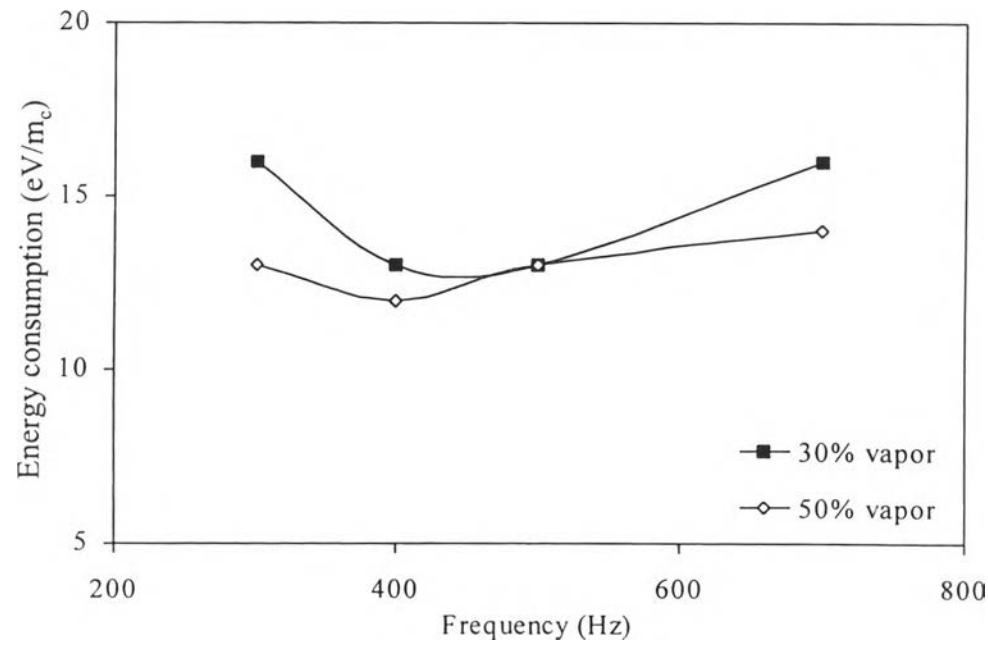

Figure 7.6 Effect of frequency on energy consumed to convert a methane molecule (conditions are the same as those in Table 7.3).

7.4.4 Effect of Residence Time

To investigate the effect of residence time, the experiments were conducted using a CH_4/O_2 ratio of 5 and water-vapor content in the feed of 30%. The effects of residence time on methane and oxygen conversions are shown in Figure 7.7. Oxygen conversion increased significantly while methane conversion slightly increased with increasing residence time. The gas residence time is related to contact time. When the residence time increases, giving a longer contact time, the collisions of gaseous molecules with sufficient energy electrons increase, resulting in higher methane and oxygen conversions. In this study, the power to initiate the reaction increases with decreasing residence time. The difference between oxygen and methane conversion increases with increasing residence time. This result implies that oxygen not only reacts with methane but also reacts with the primary products.

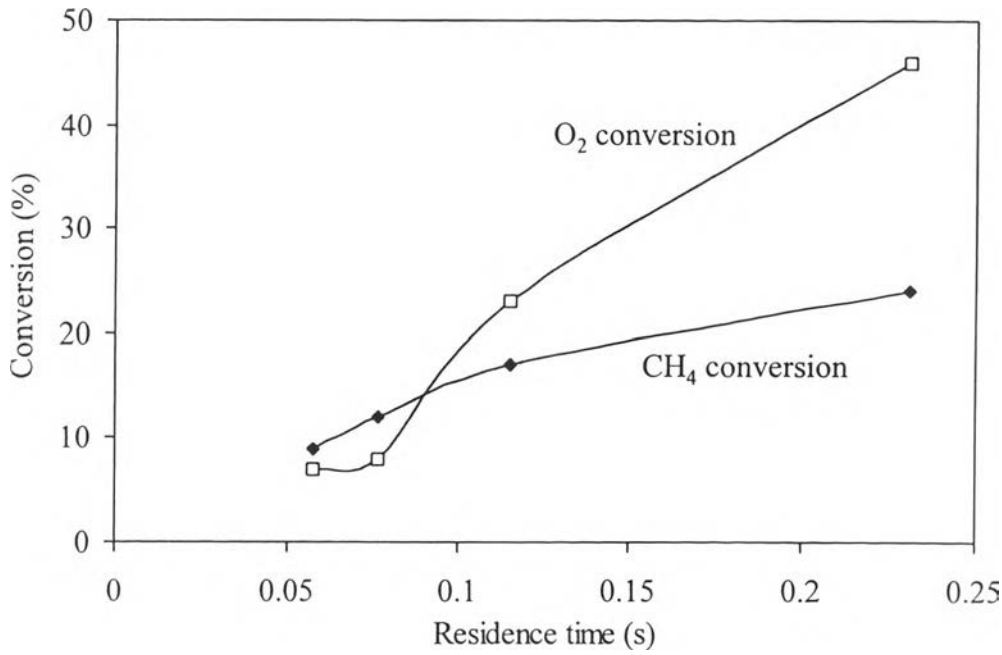

Figure 7.7 Effect residence time on conversion; gap width, 10 mm; CH_4/O_2 ratio, 5; percent water-vapor, 30; input power, 14 W; and applied frequency, 400 Hz.

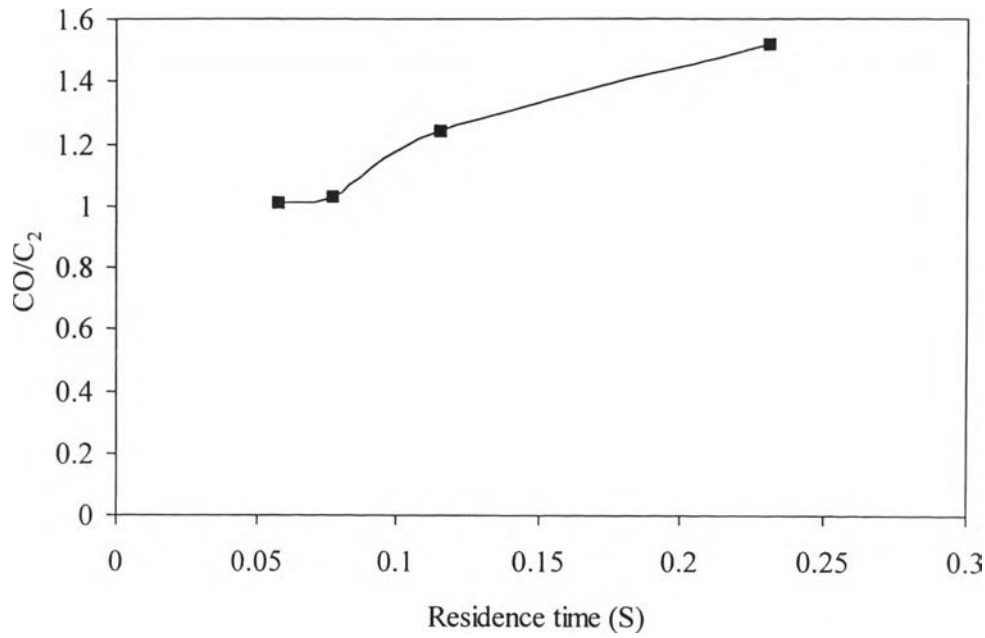

Figure 7.8 Effect residence time on CO/C_2 molar ratio; gap width, 10 mm; CH_4/O_2 ratio, 5; percent water-vapor, 30; input power, 14 W; and applied frequency, 400 Hz.

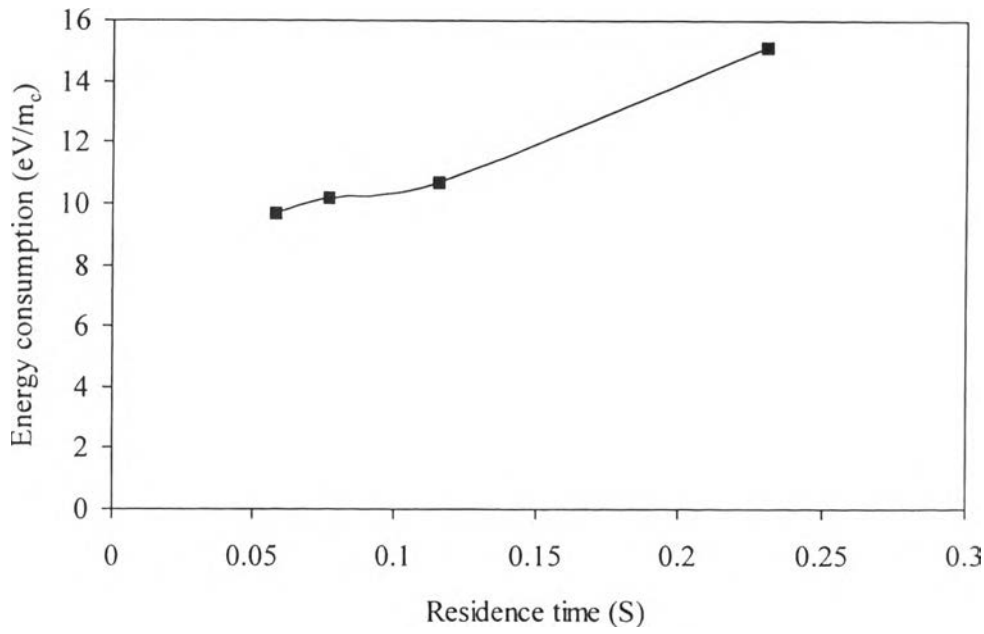

Figure 7.9 Effect residence time on energy consumed to convert a methane molecule; gap width, 10 mm; CH_4/O_2 ratio, 5; percent water-vapor, 30; input power, 14 W; and applied frequency, 400 Hz.

Figure 7.8 and Figure 7.9 show the effect of residence time on CO/C_2 molar ratio and energy consumed to convert a methane molecule, respectively. The CO/C_2 molar ratio and energy consumed to convert a methane molecule increase with increasing residence time. These results conform to the previous explanation that at longer residence time, oxygen active species also react with primary products as well as methane. At a longer residence time, these C_2 hydrocarbons have enough time to react further with oxygen to form carbon oxides. For this reason, the CO/C_2 product ratio increases with increasing residence time. Moreover, some of the energy is consumed by secondary reactions so the apparent energy consumed to convert a methane molecule increases at a longer residence times.

7.5 Conclusions

Experiments on methane reforming with water-vapor and oxygen were performed in an ac corona discharge reactor. Since water is a cheaper reactant and easy to handle, it would be useful to develop synthesis gas production using steam as a co-reactant in a low temperature methane reforming process. From the results, it was found that the coupling of methane increased with increasing CH_4/O_2 ratio if the limitation of conventional steam reforming could be overcome but the oxidation of methane to carbon oxides and water was more favorable at higher oxygen concentrations. Adding water-vapor in the feed stream greatly enhanced the conversions of methane and oxygen in an oxygen-lean system but reduced the conversion of methane in the oxygen-rich system. Moreover, the energy consumption for methane conversion could be substantially reduced by adding water-vapor at a CH_4/O_2 ratio of 5. The product distribution was strongly influenced by feed gas concentrations rather than input power and applied frequency. The methane and oxygen conversions and energy efficiency exhibited maximum values at a frequency of around 400 Hz and low frequencies results in carbon formation and loss of stability of the plasma. At the conditions studied, input power had more influence on the methane and oxygen conversions than applied frequency. With

varying residence time, the maximum energy consumed to convert a methane molecule was found at the longest residence time.

7.6 Acknowledgement

Thailand Research Fund is greatly acknowledged for supporting this work as well as providing a scholarship for the first author.

7.7 References

1 Wender, I. Reactions of Synthesis Gas. *Fuel Process. Tech.* **1996**, 48, 189.

2 Lesueur, H.; Czernichowski, A.; Chapelle, J. Electrically Assisted Partial Oxidation of Methane. *Int. J. Hydrogen Energy* **1994**, 19, 139.

3 Marchionna, M.; Lami, M.; Galletti, A. M. R. Synthesizing Methanol at Lower Temperatures. *Chemtech* **1997**, 27.

4 Armor, J. N. The Multiple Roles for Catalysis in the Production of H_2. *Appl. Catal. A* **1999**, 176, 159.

5 Tsang, S. C.; Claridge, J. B.; Green, M. L. H. Recent Advances in the Conversion of Methane to Synthesis Gas. *Catal. Today* **1995**, 23, 3.

6 Zhang, K.; Kogelschatz, U.; Eliasson, B. Conversion of Greenhouse Gases to Synthesis Gas and Higher Hydrocarbons. *Energy Fuels* **2001**, 15, 395.

7 Vernon, P. D. F.; Green, M. L. H.; Cheetham, A. K.; Ashcroft, A. T. Partial Oxidation of Methane to Synthesis Gas, and Carbon Dioxide as an Oxidising Agent for Methane Conversion. *Catal. Today* **1992**, 13, 417.

8 Han, S.; Martenak, D. J.; Palermo, R. E.; Pearson, J. A.; Walsh, D. E. Direct Partial Oxidation of Methane over ZSM-5 Catalyst: Metals Effects on Higher Hydrocarbon Formation. *J. Catal.* **1994**, 148, 134.

9 Otsuka, K.; Wang, Y.; Sunada, E.; Yamanaka, I. Direct Partial Oxidation of Methane to Synthesis Gas by Cerium Oxide. *J. Catal.* **1998**, 175, 152.

10 Tian, Z.; Dewaele, O.; Marin, G. B. The State of Rh During the Partial Oxidation of Methane into Synthesis Gas. *Catal. Lett.* **1999**, 57, 9.

11 Elmasides, C.; Kondarides, D. I.; Neophytides, S. G.; Verykios, X. E. Partial Oxidation of Methane to Synthesis Gas over Ru/TiO_2 Catalysts: Effects of Modification of the Support on Oxidation State and Catalytic Performance. *J. Catal.* **2001**, 198, 195.

12 Ji, Y.; Li, W.; Xu, H.; Chen, Y. Catalytic Partial Oxidation of Methane to Synthesis Gas over $Ni/\gamma\text{-}Al_2O_3$ Catalyst in a Fluidized-bed. *Appl. Catal. A* **2001**, 213, 25.

13 Cormier, J. M.; Rusu, Iulian. Syngas Production via Methane Steam Reforming with Oxygen: Plasma Reactors versus Chemical Reactors. *J. Phys. D: Appl. Phys.* **2001**, 34, 2798.

14 Savinov, S. Y.; Lee, H.; Song, H. K; Na, B.-K. Decomposition of Methane and Carbon Dioxide in a Radio-Frequency Discharge. *Ind. Eng. Chem. Res.* **1999**, 38, 2540.

15 Mutaf-Yardimci, O.; Saveliev, A. V.; Fridman, A. A.; Kennedy, L. A. Employing Plasma as Catalyst in Hydrogen Production. *Int. J. Hydrogen Energy* **1998**, 23, 1109.

16 Larkin, D. W.; Caldwell, T. A.; Lobban, L. L.; Mallinson, R. G. Oxygen Pathways and Carbon Dioxide Utilization in Methane Partial Oxidation in Ambient Temperature Electric Discharges. *Energy Fuels* **1998**, 12, 740.

17 Larkin, D. W.; Leethochawalit, S.; Caldwell, T. A.; Lobban, L. L.; Mallinson, R. G. Carbon Pathway, CO_2 Utilization, and In Situ Product Removal in Low Temperature Plasma Methane Conversion to Methanol. In *Greenhouse Gas Control Technologies*; Eliasson, B., Riemer, P., Wokaun, A., Eds.; Pergamon: Amsterdam, 1999; p 397.

18 Larkin, D. W.; Lobban, L. L.; Mallinson, R. G. Production of Organic Oxygenates in the Partial Oxidation of Methane in a Silent Electric Discharge Reactor. *Ind. Eng. Chem. Res.* **2001**, 40, 1594.

19 Larkin, D. W.; Zhou, L.; Lobban, L. L.; Mallinson, R. G. Product Selectivity Control and Organic Oxygenate Pathways from Partial Oxidation of Methane in a Silent Electric Discharge Reactor. *Ind. Eng. Chem. Res.* **2001**, 40, 5496.

20 Thanyachotpaiboon, K.; Chavadej, S.; Caldwell, T. A.; Lobban, L. L.; Mallinson, R. G. Conversion of Methane to Higher Hydrocarbons in ac Nonequilibrium Plasmas. *AIChE J.* **1998**, 44, 2252.

21 Yao, S. L.; Takemoto, T.; Ouyang, F.; Nakayama, A.; Suzuki, E.; Mizuno, A.; Okumoto, M. Selective Oxidation of Methane Using a Non-Thermal Pulsed Plasma. *Energy Fuels* **2000**, 14, 459.

22 Zhou, L. M.; Xue, B.; Kogelschatz, U.; Eliasson, B. Nonequilibrium Plasma Reforming of Greenhouse Gases to Synthesis Gas. *Energy Fuels* **1998**, 12, 1191.

23 Chang, J.-S.; Lawless, P. A.; Yamamoto, T. Corona Discharge Processes. *IEEE Trans. Plasma Sci.* **1991**, 19, 1152.

24 Liu, C.; Marafee, A.; Hill, B.; Xu, G.; Mallinson, R.; Lobban, L. Oxidative Coupling of Methane with ac and dc Corona Discharges. *Ind. Eng. Chem. Res.* **1996**, 35, 3295.

25 Liu, C.; Mallinson, R.; Lobban, L. Nonoxidative Methane Conversion to Acetylene over Zeolite in a Low Temperature Plasma. *J. Catal.* **1998**, 179, 326.

26 Sorensen, S. L.; Karawajczyk, A.; Stromholm, C.; Kirm, M. Dissociative Photoexcitation of CH_4 and CD_4. *Chem. Phys. Lett.* **1995**, 232, 554 .

27 Eliasson, B.; Kogelschatz, U. Nonequilibrium Volume Plasma Chemical Processing. *IEEE Trans. Plasma Sci.* **1991**, 19, 1063.

28 Grill, A. *Cold Plasma in Materials Fabrication, From fundamentals to applications*; IEEE Press: New York, 1994.

29 Liu, C.; Marafee, A.; Mallinson, R.; Lobban, L. Methane Conversion to Higher Hydrocarbons in a Corona Discharge over Metal Oxide Catalysts with OH Groups. *Appl. Catal. A* **1997**, 164, 21.